

Experimental Study of the Impact Damage of Composition B and Plastic Bonded Explosive

CHEN Peng-wan(陈鹏万)¹, HUANG Feng-lei(黄风雷)¹, DING Yan-sheng(丁雁生)²

(1. State Key Laboratory of Explosion and Safety Science, Beijing Institute of Technology, Beijing 100081, China;

2. Institute of Mechanics, Chinese Academy of Sciences, Beijing 100080, China)

Abstract: A long-pulse low-velocity gas gun with a gas buffer is used to induce impact damage in cast Composition B and hot pressed PBXN-5. To obtain different damage states, a range of projectile velocities are used by controlling the launching pressure of gas gun. The stress history during impact loading is recorded. Various methods are used to characterize the damage state of impacted explosive samples. The microstructure is examined by use of scanning electronic microscopy (SEM) and polarized light microscopy (PLM). The densities and ultrasonic attenuation are also measured. The results show that both Composition B and PBXN-5 exhibit some damage characteristics of brittle materials. However, due to the difference in compositions, PBXN-5 exhibits better resistance to impact loading than Composition B.

Key words: explosives; impact damage; microstructure; ultrasonic attenuation

CLC number: O 344.6; TQ 560.71 **Document code:** A **Article ID:** 1004-0579(2003)03-0273-05

Explosives may be subject to shake, impact or shock in manufacturing, transportation, storage, launching and penetration. Dynamic loading will, in return, induce different forms of damage including microcracks, microvoids, crystal fractures and even some chemical reaction. Damage not only deteriorates the mechanical properties of explosives, but also influences the sensitivity, combustion and even detonation behavior of explosives. Damaged energetic materials have higher risks of the formation of hot spots, combustion abnormality and even deflagration to detonation (DDT)^[1-3]. It is recognized that damaged energetic materials are more vulnerable to external solicitations. Delayed detonation (XDT) remains to be a top concern for a long period in this regard.

The responses of explosives to dynamic loading are extremely complex, involving a coupling of mechanical, thermal and chemical responses. The characterization of the damage state, including the size, number and distribution of microcracks and other

forms of damage, and their evolution law is a key to the study of dynamic damage. The low strengths and risks of combustion and explosion bring additional difficulties to the study of mechanical damage of explosive materials. Drop weight can be used to produce damage at median level strain rates^[2-3]. The damage produced at high strain rates can be achieved with high-speed projectiles and flying plates^[4-6]. When conventional gas guns and explosive-driven flying plates are used in dynamic loading, it is generally difficult to control the stress amplitude and duration of dynamic load, thus to control the damage extent. To overcome this, we developed a long-pulse low-velocity gas gun with a gas buffer. In this paper, we use this gas gun to apply dynamic load and induce impact damage. The explosives used include cast Composition B and a hot pressed plastic bonded explosive (PBX). Microscopic examination, density and ultrasonic attenuation measurement are carried out to characterize the damage state of impacted explosives.

Received 2002-07-09

Sponsored by the National Natural Science Foundation (10002022) and Joint Foundation of Chinese Natural Science Committee and Chinese Academy of Engineering Physics (10076021)

Biography CHEN Peng-wan(1971-), associate professor, Ph. D., pwchen@bit.edu.cn.

1 Experiment

Cast Composition B and hot pressed PBXN-5 are used in the experiment in order to evaluate the influences of composition and shaping methods. Composition B contains TNT 40.0% and RDX 60.0%. PBXN-5 contains HMX 94.5%–95.0% and fluorin rubber 5.0%–5.5%. The pressing pressure and temperature are 200 MPa and 100 °C and the duration of pressing is 1.5 h.

The gas gun used in our experiment is developed to apply long-pulse dynamic loading. The diameter of the gas gun is 56 mm. To extend the duration of dynamic loading, a gas buffer is developed and installed on the gun. The duration of dynamic loading can be adjusted by filling the buffer with different pressures of gas. The duration of direct impact between two metal plates usually lasts only about hundreds of microseconds. However this can be extended to several milliseconds by use of a gas buffer. The impact velocities are controlled not to detonate the samples in order to examine the evolution of microstructure.

Figure 1 is a schematic diagram of impact loading. The sample is constrained in a steel tube. Two polyethylene cushions are placed between the explosive sample and two steel rods. The diameter and length of projectiles are 56 mm and 110 mm. Both steel projectiles and aluminum projectiles are used. The weight of a steel projectile and an aluminum projectile are 2.00 kg and 0.72 kg respectively. A stress gauge is mounted on steel rod 1 to measure the stress history during impact. The sample sizes for PBXN-5 and Composition B are $\varnothing 20 \text{ mm} \times 10 \text{ mm}$ and $\varnothing 20 \text{ mm} \times 20 \text{ mm}$ respectively.

Different methods are used to characterize impact

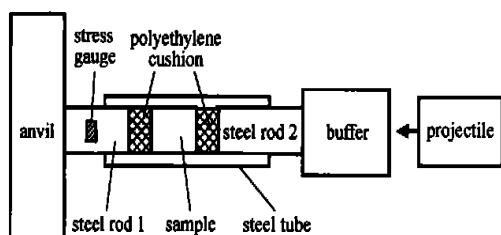


Fig. 1 Schematic diagram of dynamic loading

induced damage. The sample densities before and after impact are measured by using Archimedes method. Scanning electronic microscopy (SEM) and polarized light microscopy (PLM) are used to examine the microstructural evolution under impact loading. An explosive usually has an exceptionally low toughness. Palmer and Field^[7], for instance, quoted a toughness of $0.05 \text{ MN} \cdot \text{m}^{-3/2}$ for PBX9501, four orders of magnitude smaller than typical engineering alloys. In addition, explosive materials have risks of combustion and explosion. These bring difficulties to the preparation of microscopic samples. In our experiment, samples are first ground with standard fine silicon carbide papers (800 grid) to obtain a flat surface. Final polishing is carried out in an automatic polishing machine with 1 μm alpha alumina powder, at a load of 50 g, while being lubricated with distilled water. To avoid bringing additional unexpected damage to impacted samples in polishing, samples are first potted in commercial low-viscosity epoxide mounts with traditional amine hardening agent and then cured. To better reveal the details of the microstructure, isomethyl butyl ketone is selected to etch the surface. The polished and etched samples are directly used for PLM examination, while they have to be coated with a thin layer of gold for SEM examination. The whole polishing process can be monitored by using a CCD camera. To avoid the accumulation of friction heat and causing fatal accident in the polishing process, continuous distilled water is required to cool the samples. Figure 2 shows a schematic description of an impact damaged sample. Three representative fields including near-field (A), mid-field (B) and far-field (C), are chosen for examination.

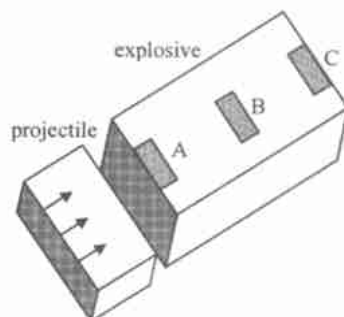


Fig. 2 Schematic of view fields

Ultrasonic attenuation is measured before and after impact by use of pulse through-transmission method⁸, in which water is used as a coupling medium. The attenuation coefficient is calculated by

$$\alpha = \frac{20}{d} \left[\lg \frac{A}{A_0} - \lg \frac{(\rho c + \rho_w c_w)^2}{4 \rho c \rho_w c_w} \right], \quad (1)$$

where α is the attenuation coefficient, d is the thickness of samples, A_0 and A are the amplitudes of ultrasonic wave pulses before and after inserting samples into water, ρ and c are the density and sound velocity of samples, ρ_w and c_w are the density and sound velocity of water.

2 Results and Discussion

Figure 3 shows a recorded stress history of PBXN-5 sample impacted by a steel projectile at a velocity of 109.0 m/s. The peak stress and duration of stress impulse are about 264 MPa and 3 ms respectively. It is clear that the buffer plays an important role in extending the duration one order higher than usual. Figure 4 is a micrograph of undamaged PBXN-5, showing some microcracks in explosive particles as a result of hot pressing. Figures 5—7 are plan-view images of damaged PBXN-5 impacted at a speed of 109.0 m/s. Figure 5 is an image of near-field, while

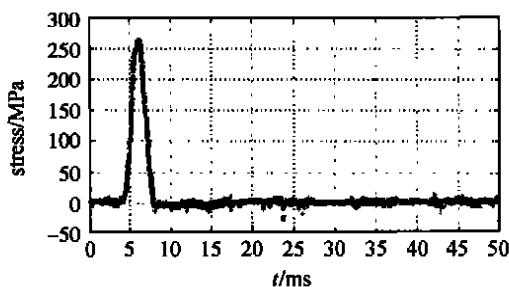


Fig. 3 A typical stress history of impact loading

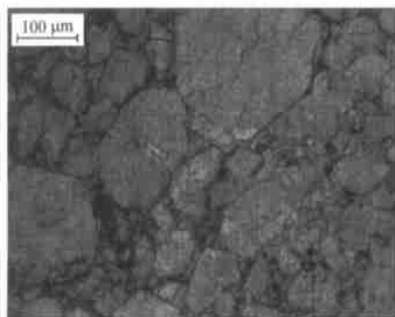


Fig. 4 Plan view of undamaged PBXN-5

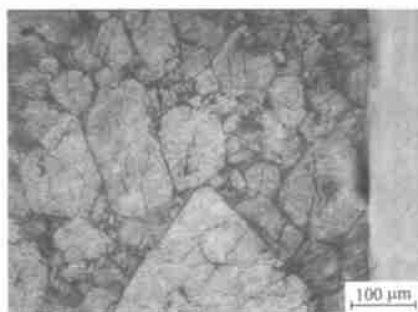


Fig. 5 Near-field region, damaged PBXN-5

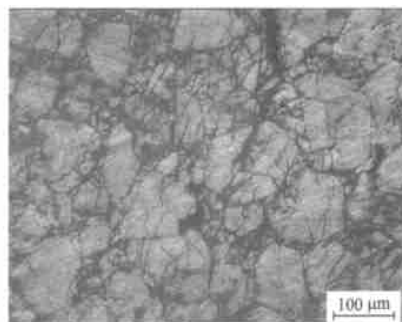


Fig. 6 Mid-field region, damaged PBXN-5

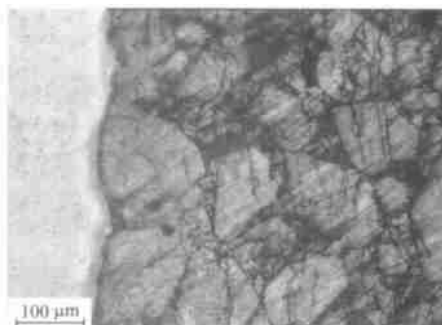


Fig. 7 Far-field region, damaged PBXN-5

Fig. 6 and Fig. 7 are mid-field and far-field respectively, with the projectile incident from right (The incident direction in Fig. 8 and Fig. 9 are the same). The damaged PBXN-5 shows more microcracks than undamaged samples. The mid-field and far-field regions show even more particle fracture than near-field region. A larger crack is present in mid-field region, showing the coalescence of microcracks. Some transgranular cracks can be clearly seen in the micrographs.

Figure 8 and Fig. 9 are images of near-field and far-field of damaged Composition B impacted under the same condition. Though some transgranular microcracks are also present in RDX particles, the

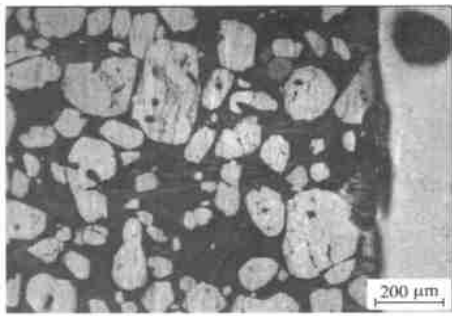


Fig. 8 Near-field region, damaged Composition B

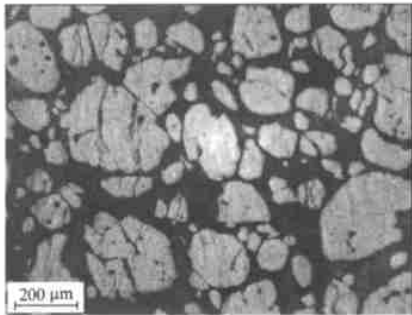


Fig. 9 Far-field region, damaged Composition B

number of microcracks and fractured explosive particles is much lower than damaged PBXN-5 samples. It is worthwhile to note that the substantial preferred orientation of the microcracks and the coalesced crack in mid-field and far-field is in the vertical direction for both PBXN-5 and Composition B samples. Figure 10 is a fractograph of Composition B, demonstrating that intergranular fractures are the main fracture mode for Composition B. Some extruding RDX particles and some pits due to the pulling out of RDX particles can be clearly seen in the picture.

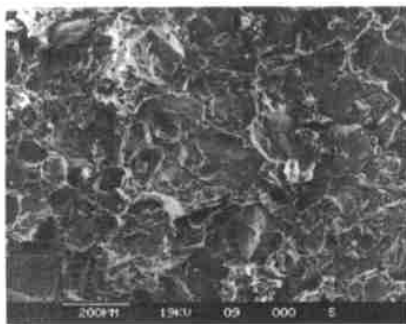


Fig. 10 A typical fractograph of damaged and fractured Composition B

Few visible cracks can be observed in damaged

PBXN-5 impacted by a steel projectile at a speed of 109 m/s. However several visible through cracks vertical to incident direction are present in damaged Composition B impacted under the same condition, and some large fragmentations on the opposite side of impact plane are produced. The results show that PBXN-5 possesses better resistance to impact loading, while Composition B is more brittle than PBXN-5. The composition difference between the two explosives may be the main reason for the results. Both RDX and TNT crystals in Composition B are brittle. Though the viscoelastic binder content in PBXN-5 is relatively low, only about 5%, it still enhances the resistance of the whole material to mechanical loading noticeably.

Table 1 shows the density variation before and after impact under different impact conditions. Due to the formation of extensive microcracks, the densities in damaged samples are reduced. The higher the impact stress is, the more the density reduces. When PBXN-5 samples are impacted by aluminum projectiles at speeds of 60.4, 125.4, 147.8, 191.4 and 194.1 m/s, the densities decrease by 0.214%, 0.273%, 0.525%, 1.082% and 1.114% respectively. When the samples are impacted by a steel projectile at a speed of 109.0 m/s, the densities of PBXN-5 and Composition B decrease by 1.820% and 0.420% respectively. Table 2 lists the ultrasonic attenuation coefficients of undamaged and damaged samples. It is also shown that higher impact velocities and shock stress cause more severe damage and larger ultrasonic attenuation. The attenuation coefficient of undamaged PBXN-5 is 2.60 dB/mm. But the attenuation coefficients of the damaged samples impacted by aluminum projectiles at speeds of 60.4, 125.4, 147.8 and 191.4 m/s increase to 2.85, 3.55, 4.67 and 4.72 dB/mm, showing an increase of 9.6%, 36.5%, 79.6% and 81.5% respectively. The results demonstrate that the variation of attenuation coefficient is much larger than the density for impact damage. The ultrasonic attenuation coefficient seems to be a more sensitive variable than density.

Tab. 1 Density variation of undamaged and damaged explosives

materials	$\Delta\rho/\%$					
	projectile velocity/($\text{m}\cdot\text{s}^{-1}$)/ peak stress/MPa					
	60. 4/ 56. 3	125. 4/ 113. 3	147. 8/—	191. 4/ 212. 5	194. 1/—	109. 0/— *
PBXN-5	-0. 214	-0. 273	-0. 525	-1. 082	-1. 114	-1. 820(264 MPa)
Comp B	—	—	—	—	—	-0. 420(283 MPa)

*steel projectiles, the rest are aluminum projectiles

Tab. 2 Attenuation coefficients of undamaged and damaged explosives

acoustic properties	undamaged	projectile velocity/($\text{m}\cdot\text{s}^{-1}$)/ peak stress/MPa			
		60. 4/ 56. 3	125. 4/ 113. 3	147. 8/—	191. 4/ 212. 5
attenuation/($\text{dB}\cdot\text{mm}^{-1}$)	2. 60	2. 85	3. 55	4. 67	4. 72

3 Conclusions

The long-pulse low-velocity gas gun used in our experiment proves to be an efficient loading apparatus in the study of dynamic damage and mechanical properties of explosive materials. Both PBXN-5 and Composition B exhibit damage characteristics of brittle materials. Impact induces a large number of microcracks, which causes the density to decrease and ultrasonic attenuation to increase. Higher projectile velocity and higher impact stress cause a larger extent of damage, a lower density and a larger attenuation coefficient. Composition B appears to be more brittle than PBXN-5. The composition difference between them may account for that. A few percent of binder in PBXN-5 can noticeably enhance the resistance of the whole material to impact loading.

The impact stress generated in our experiment is not high enough to induce chemical reaction in damaged explosives. To characterize the microstructure of explosives with local impact-induced chemical reaction, larger projectile velocities or a gas gap are planned to be used for further study. This may deepen our understanding of the formation mechanisms of hot spots under impact loading.

References:

[1] Huang Fenglei, Bai Chunhua, Ding Jing. Shock initia-

tion of damaged solid propellant[J]. China Safety Science Journal, 1994, 4(4): 1—5. (in Chinese)

[2] Zhang Taihua. Damage of a propellant and its stability of combustion [D]. Beijing: Institute of Mechanics, Chinese Academy of Sciences, 1999. (in Chinese)

[3] Demol G, Lambert P, Trumel H. A study of the microstructure of pressed TATB and its evolution after several kinds of solicitations[A]. Short J M, Kennedy J E. Papers Summaries—Eleventh International Detonation Symposium[C]. Snow mass: [s. n.], 1998. 404—406.

[4] Green L, James E, Lee E. Energetic response of propellants to high velocity impact[A]. Short J M. Proceedings of Eighth Symposium (International) on Detonation[C]. Albuquerque, New Mexico: [s. n.], 1985. 284—293.

[5] Zhao Feng, Sun Chengwei, Wen Shanggang, et al. Brittle fracture of high explosive JO-9159 under plate impact loading[J]. Explosion and Shock Waves, 2001, 21(2): 121—125. (in Chinese)

[6] Sandusky H W, Bernerker R R. Influence of fresh damage on the shock reactivity and sensitivity of several energetic materials[A]. Short J M, Tasker D G. Proceedings of Tenth Symposium (International) on Detonation[C]. Boston, Massachusetts: [s. n.], 1993. 490—498.

[7] Palmer S J P, Field J E. The deformation and fracture of beta-HMX[J]. Proc R Soc Lond, 1982, A383: 399—407.

[8] Zhu Chenggang, Cheng Yang, Niu Fengqi. Investigation of limiting factors in the ultrasonic attenuation measurements by using the pulse through-transmission method [J]. Acta Acustica, 2002, 27(3): 249—252. (in Chinese)